

α Centauri revisited: 2nd epoch ALMA observations

R. Liseau

Department of Earth and Space Sciences, Chalmers University of Technology, Onsala Space Observatory, SE-439 92 Onsala, Sweden,
e-mail: rene.liseau@chalmers.se

Received ; accepted

ABSTRACT

Context. The observational study of stars in the sub-millimetre regime has only rather recently begun and was made possible mainly by the Atacama Large Millimeter/submillimeter Array (ALMA). The emission mechanisms of this radiation from normal Main-Sequence stars and its physical significance for the outer atmospheric layers is the topic of intense contemporary study.

Aims. Our previous ALMA observations of the α Centauri binary system detected the submm emission originating in the chromospheres of these solar-type stars. Observations at another epoch are aiming at further characterising these atmospheric layers and their behaviour with time. In addition, we were aiming at clarifying the status of the recently discovered U source and its relation to the α Cen system.

Methods. The comparison of data from two epochs should present the basis for more advanced theoretical modelling of the chromospheres of α Cen A and B. Proper motion data of the U source should establish its relation to the α Cen system, and U's submm spectral energy distribution (SED) should provide information about its physical nature.

Results. In Cycle 4, both stars were again detected in the same bands as in the earlier Cycle 2. These early data suggested a flattening of the SED towards longer wavelengths. By analogy with the Sun, this was not expected. Eventually, it turned out to be caused by an obsolete calibration, but this has now been remedied. Each SED exhibits now a single spectral slope over the entire frequency range (90 to 675 GHz). For the U source, the upper limits on its proper motion (pm) are much smaller than the pm of α Cen, which essentially excludes any physical relationship with the binary.

Conclusions. The second epoch ALMA observations of α Cen did not confirm the flattening of the SED in the lowest frequency bands that was reported before. Rather, this was the result of an inadequate flux calibration using the minor planet Ceres. Over the entire frequency range observed with ALMA, the SEDs from Cycle 4 can be fit by power laws of the form $S_\nu \propto \nu^\alpha$ with $\alpha = 1.76 \pm 0.01$ for α Cen A and $\alpha = 1.71 \pm 0.02$ for α Cen B. For the infrared/submm background object U applies $\alpha = 2.55 \pm 0.14$. If this emission from U is due to dust, its opacity exponent $\beta = \alpha - 2$ would be about 0.5, indicative of particle sizes that are larger than those of the interstellar medium ($\beta_{\text{ISM}} \sim 2$), but comparable to those found in circumstellar discs.

Key words. stars: solar-type – (stars:) binaries: general – stars: individual: α Centauri AB – submillimeter: stars

1. Introduction

During ALMA-Cycle 2, Alpha Centauri (α Cen) has been observed in 2014 and 2015. The results of these successful observations have been communicated by Liseau et al. (2015) and Liseau et al. (2016). For the further study of the chromospheric emissions from the binary stars, a new observing campaign was initiated during Cycle 4 (2016 - 2017), again exploiting all of the previously available frequency bands, i.e. bands 3, 4, 6, 7, 8 and 9 in the range 90 to 675 GHz (3 to 0.4 mm). This generated second epoch datasets for the study of the chromospheres of the G2 V (α Cen A) and K1 V star (α Cen B) and of the nature of the mysterious and unidentified object U, then situated about 5'' north of A. The discovery of U was reported in the 2016 paper.

In the next section, Sect. 2, we will discuss the new observations and the data reduction, with particular emphasis on the calibrations. The results for α Cen A and B are provided in Sect. 3, which are discussed in Sect. 4. In Sect. 5, we turn our attention toward the U source. Finally, in Sect. 6, we briefly present our main conclusions.

2. Observations and data reduction

The observations of Cycle 2 (C2, ID 2013.1.00170.S) have already been described and analysed by Liseau et al. (2015) and

Liseau et al. (2016) and will not be repeated here, unless required by the context, (see, e.g., the upper half of Table 1).

The Cycle 4 (C4, ID 2016.1.00441.S) observations using the number of antennas shown in the lower half of Table 1 were performed during 2016 and 2017. Due to phase errors in the Band 3 and 4 observations, these data had to be re-acquired, which resulted in the delayed access to the data. For all observations, the number of telescopes was larger during C4 and, therefore, a higher sensitivity, by about 25% to 40%, could be expected. The parameters of the synthesised beams are also provided in that table, where a and b refer to the major and minor axes, respectively, of the elliptical Gaussian beam at half power.

The selection of the ALMA configuration, i.e. the maximum extent of the baselines, should ensure that the stars, having apparent diameters less than 10 mas, would remain spatially unresolved at all observing frequencies. As a result, the observation of point sources should render the reduction of the interferometric data relatively straightforward, using a source model corresponding to the synthesised elliptical Gaussian telescope beam to obtain best-fits to the observed visibilities.

Table 1. Instrumental parameters for Cycles 2 and 4, respectively

Cycle	Obs. Date	N	Synth. Beam	PA
Band	yyyy-mm-dd	Ant.	$a \times b (")^2$	($^\circ$)
C2				
3	2014-07-03	30	1.81×1.22	19
7	2014-07-07	32	0.43×0.28	47
9	2014-07-18	31	0.22×0.16	36
6	2014-12-16	35	1.64×1.07	71
4	2015-01-18	34	3.16×1.67	82
8	2015-05-02	37	0.77×0.68	-70
C4				
4	2016-12-19	42	1.38×1.01	-25
6	2016-12-30	44	0.81×0.70	-50
9	2017-03-22	42	0.67×0.51	60
7	2017-03-26	43	1.28×1.08	41
8	2017-04-07	43	1.08×0.97	51
3	2017-05-08	47	0.73×0.50	-28

Table 2. ALMA calibration for Cycles 2 and 4

Obs. Date	Calibration: Sources and Functionality		
	Phase	Bandpass	Flux
yyyy-mm-dd			
C2			
Bd			
3	2014-07-03	J1617-5848	J1427-4206 Ceres
7	2014-07-07	J1617-5848	J1427-4206 Titan
9	2014-07-18	J1617-5848	J1508-4953 Ceres
6	2014-12-16	J1408-5712	J1427-4206 J1427-421
4	2015-01-18	J1617-5848	J1617-5848 Ceres
8	2015-05-02	J1617-5848	J1427-4206 Titan
C4			
Bd			
4	2016-12-19	J1424-6807	J1617-5848 Ganymed
6	2016-12-30	J1424-6807	J1617-5848 Callisto
9	2017-03-22	J1424-6807	J1266-0547 Titan
7	2017-03-26	J1427-4206	J1424-6807 Titan
8	2017-04-07	J1424-6807	J1617-5848 Callisto
3	2017-05-08	J1424-6807	J1617-5848 J1617-5848

3. ALMA Data Calibration

The visibilities were calibrated following standard procedures using the CASA package (Common Astronomy Software Application, version 5.1.1). The calibration sources and their functions during our 2014/15 and 2016/17 observing campaigns, respectively, are shown in Table 2. For complex gain calibration and bandpass, quasars were generally used. These are listed in the table under “Phase” and “Bandpass”, respectively. Flux calibration was achieved by mostly observing asteroids and moons in the solar system, but occasionally quasars were also used (see column “Flux” in Table 2).

The C2 observations were all re-reduced in the same way as those of C4. That should guarantee an overall homogeneous data set for both cycles (see, e.g., Table 3).

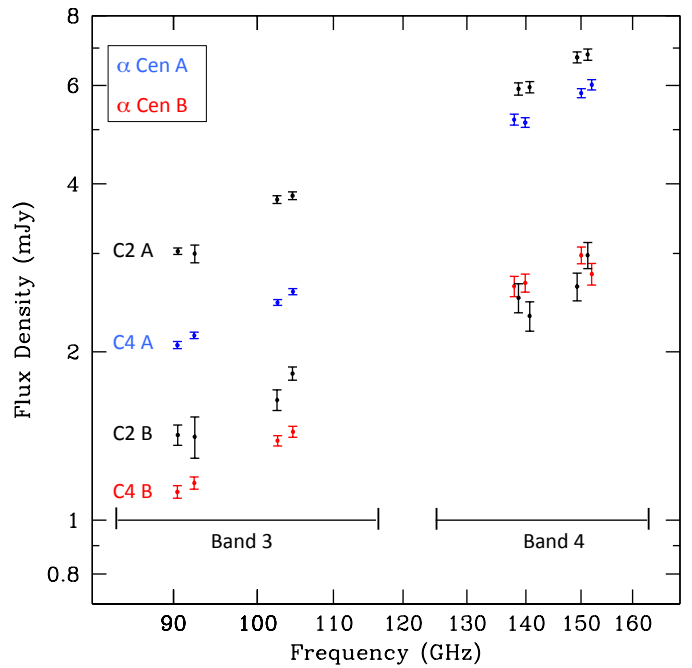


Fig. 1. ALMA Band 3 and 4 flux densities of α CenA and B during two observing cycles (C2 and C4). The four individual sub-band fluxes (2 GHz/spw) in a given band are shown, where black indicates C2 data of both stars. Re-calibrations are shown in blue for α CenA and in red for the cooler α CenB. Shown errors are statistical only. Regarding absolute levels, see the text (Sect. 3.2).

Table 3. Cycle 2: Ceres calibration of α CenA and α CenB

Band 3: $S_{97.5\text{GHz}}$ (mJy)	Band 4: $S_{145\text{GHz}}$ (mJy)
Cycle 2	
A: 3.37 ± 0.01 [S/N=281]	6.33 ± 0.08 [S/N=83]
B: 1.59 ± 0.02 [S/N= 80]	2.58 ± 0.08 [S/N=34]
Cycle 4	
A: 3.159 ± 0.016 [S/N=197]	5.255 ± 0.037 [S/N=142]
B: 1.549 ± 0.016 [S/N= 97]	2.481 ± 0.042 [S/N= 59]

3.1. Flux calibration with Ceres

From the Cycle 2 data, it came as a complete surprise that the spectral energy distribution (SED) appeared to change slope at the lowest ALMA frequencies, viz. in bands 3 and 4 (Liseau et al. 2016).

Based on the solar analogy, one would have expected this not to happen before at much lower frequencies, i.e. in the radio regime. In the paper by Liseau et al. (2016, Table 2), the data for Bands 3 (2014-07-03) and 4 (2015-01-18) have been calibrated with an obsolete model for the asteroid Ceres. These observations took place before January 2015, and a Ceres model with a constant brightness temperature with frequency (185 K) was used. Thereafter, thermo-physical models have been applied (Butler 2012, see also: Appendix C in the CASA User Manual, https://casa.nrao.edu/docs/UserMan/casa_cookbook014.html).

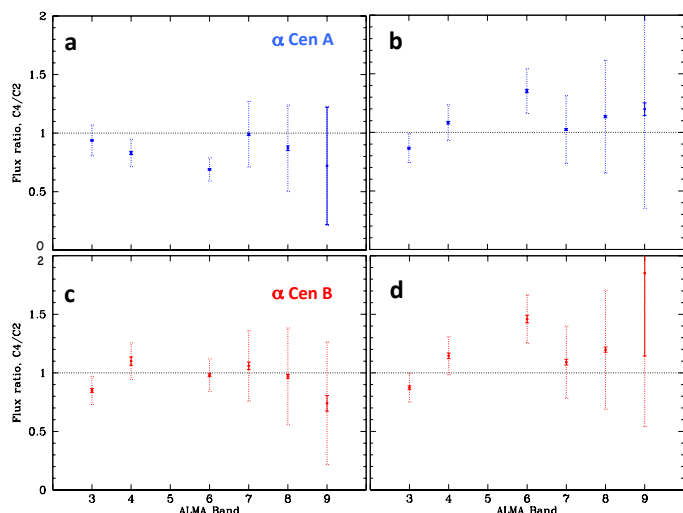


Fig. 2. Ratio of band-integrated flux densities obtained for α CenA (blue) during Cycle C2 in **a** and C4 in **b**. Similar for α CenB (red) in **c** and **d**, respectively. In **a** and **c**, the C2 fluxes are those published by Liseau et al. (2016), whereas in **b** and **d**, the C2 fluxes are the re-reduced ones, i.e. those of Tables 4 and 5. The dotted lines are based on the estimates of the absolute uncertainties according to Butler (2012), and computed for independent measurements with individual errors ∂S_ν , i.e. $\Delta R_\nu = \pm R_\nu \sqrt{(\partial S_{\nu,C4}/S_{\nu,C4})^2 + (\partial S_{\nu,C2}/S_{\nu,C2})^2}$, where $R_\nu \equiv S_{\nu,C4}/S_{\nu,C2}$.

3.2. Absolute flux calibration

In order to determine absolute fluxes, the absolute systematic uncertainties need to be assessed and accounted for: currently, estimates and goals place these at better than 10% in B3 (calibration from the quasar J1617-5848), and according to Butler (2012) better than 5-10% in B4 (calibration from Ganymede), better than 10% in B6 (calibration from Callisto), perhaps better than 20% in B7 (calibration from Titan, no spectral lines), better than 30% in B8 (calibration from Callisto) and maybe better than 30-50% in B9 (calibration from Titan, no spectral lines).

The comparison of the absolute flux densities derived for the C4 data with those of C2 (both previous and current) is shown in Fig. 2.

4. Results

Also in Cycle 4, both stars, α Cen A and α Cen B, were detected at high signal to noise. As expected, the reconstructed stellar images were those of point sources outlining the synthesized elliptical telescope beams at the different frequencies. The adopted flux calibrations resulted in the values displayed in Tables 4 and 5.

For α Cen A, the results are presented in Table 4 which contains the data for both the re-reduced C2 and C4, ordered chronologically. The first column, designated Bd, shows the ALMA band identification, the frequency of which is given in column two. The Gregorian observing date and the Modified Julian Date follow, where $\text{MJD} = \text{JD} - 2400000.5$. The measured J2000.0 equatorial coordinates (ICRS) with their error estimates are listed in columns 5 to 8. Finally, the flux densities and their statistical errors are found in columns 9 and 10. The corresponding information for α Cen B is given in Table 5.

Prior to 2015, Band9 observations (2014-07-18) were also flux calibrated using Ceres and also showed over-estimated flux densities compared to those taken in 2017-03-22. However,

given the absolute uncertainties of up to 30-50% in Band 9 (calibration from Titan), this mismatch is formally within the errors.

4.1. The SEDs of α CenA and B

At the lower frequencies, the SEDs follow essentially the same trend as that determined at higher frequencies, i.e. exhibiting $S_\nu \sim \nu^\alpha$ over nearly two orders of magnitude in flux density (cf. Fig. 3). For instance, α equals two for blackbody, i.e. optically thick, radiation in the Rayleigh-Jeans regime.

Linear regression (Press et al. 1986) of the C4 Band 3 to 9 data results in $d \log S_\nu / d \log \nu = 1.76 \pm 0.01$ for α CenA and 1.71 ± 0.02 for α CenB, respectively (Fig. 3). The SEDs appear flatter than those of blackbodies and also of what was obtained before. However, the results of the 2016 paper seem less significant. Clearly, with the current uncertain status of the absolute intensity calibration, our monitoring can at present not be used to meaningfully assess the level of stellar variability of α Cen in the submm (see Fig. 2).

4.2. The sky motions of the stars α CenA and B

The positional measurements of the components of the α Cen binary, together with the graphical representation of their ephemerides, are shown in Fig. 4. These data are also provided in Tables 4 and 5. The ephemerides were calculated adopting the stellar data from Kervella et al. (2016). Included in the ephemeris computations are the contributions from the orbital motions, the annual parallaxes and the proper motions of the binary stars, leading to complex patterns as shown in Fig. 4. The agreement of the theoretical results with the observational data is generally satisfactory.

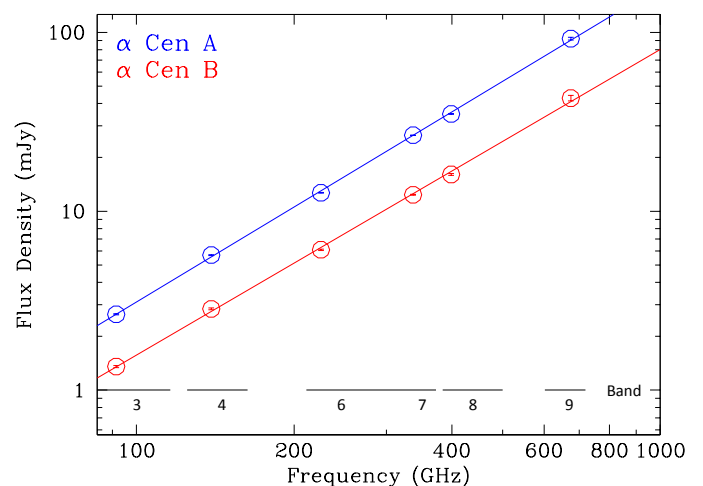


Fig. 3. Band integrated flux densities in mJy as function of the frequency in GHz of α Cen A (blue symbols) and α Cen B (red symbols) obtained during Cycle 4. These were integrated over the ALMA bands, which are indicated below. The straight lines are fits to the logarithmic data and have slopes of about 1.7 (see Sect. 4.1). The data points and their errors, which result from the fitting of the observed visibilities, are shown inside the large circles.

5. The nature of the U source

5.1. The ephemerides of U

In Fig. 4 also the corresponding data for the U source are shown, in black for the C2 and in green for the C4 observations. The

Table 4. ALMA observations of α Cen A during 2014 - 2017

Bd	ν	Obs. Date	MJD	RA (J2000)	δ_{RA}	Dec (J2000)	δ_{Dec}	S_{ν}	δS_{ν}
	GHz	yyyy mm dd	JD - 2400000.5	14 h 39 m + s	s	$-(60^{\circ} 49' +'')$	"	mJy	mJy
3	91.487	2014 07 03	56841.0557552	28.800	0.0004	58.14	0.003	3.159	0.016
7	337.487	2014 07 07	56845.1131701	28.802	0.0003	58.18	0.002	25.989	0.191
9	675.002	2014 07 18	56856.0551458	28.777	0.0004	58.08	0.003	76.945	1.647
6	224.992	2014 12 16	57007.4699005	28.716	0.0008	57.61	0.004	9.373	0.082
4	138.987	2015 01 10	57040.5804693	28.663	0.0014	57.99	0.006	5.255	0.042
8	398.987	2015 05 02	57144.1387865	28.455	0.0003	58.29	0.002	30.850	0.175
4	138.987	2016 12 19	57741.4962025	27.654	0.0005	56.78	0.004	5.685	0.037
6	224.992	2016 12 29	57752.4800353	27.636	0.0003	56.79	0.002	12.675	0.063
9	675.002	2017 03 21	57834.3408501	27.511	0.0007	57.42	0.005	92.226	1.542
8	398.987	2017 03 26	57838.2734034	27.499	0.0004	57.46	0.003	34.969	0.188
7	337.487	2017 03 26	57838.2947216	27.498	0.0003	57.38	0.002	26.608	0.075
3	91.487	2017 05 07	57881.1324039	27.374	0.0003	57.41	0.003	2.652	0.019

Table 5. ALMA observations of α Cen B during 2014 - 2017

Bd	ν	Obs. Date	MJD	RA (J2000)	δ_{RA}	Dec (J2000)	δ_{Dec}	S_{ν}	δS_{ν}
	GHz	yyyy mm dd	JD - 2400000.5	14 h 39 m + s	s	$-(60^{\circ} 49' +'')$	"	mJy	mJy
3	91.487	2014 07 03	56841.0557552	28.252	0.0004	57.14	0.003	1.549	0.016
7	337.487	2014 07 07	56845.1131701	28.240	0.0003	57.28	0.002	11.322	0.248
9	675.002	2014 07 18	56856.0551458	28.216	0.0004	57.16	0.003	23.150	0.825
6	224.992	2014 12 16	57007.4699005	28.743	0.0008	56.41	0.004	4.171	0.083
4	138.987	2015 01 10	57040.5804693	28.163	0.0014	56.44	0.006	2.481	0.042
8	398.987	2015 05 02	57144.1387865	27.943	0.0003	56.80	0.002	13.404	0.188
4	138.987	2016 12 19	57741.4962025	27.259	0.0005	53.85	0.004	2.844	0.035
6	224.992	2016 12 29	57752.4800353	27.244	0.0003	53.83	0.002	6.089	0.056
9	675.002	2017 03 21	57834.3408501	27.134	0.0007	54.26	0.005	42.870	1.534
8	398.987	2017 03 26	57838.2734034	27.125	0.0004	54.30	0.003	16.050	0.188
7	337.487	2017 03 26	57838.2947216	27.124	0.0003	54.24	0.002	12.352	0.076
3	91.487	2017 05 07	57881.1324039	27.009	0.0003	54.16	0.003	1.354	0.019

source was firmly discovered in Band 8 in 2015, only some $5''$ north of α Cen A (Liseau et al. 2016). At the distance of the solar sibling, this would correspond to a projected orbit midway between Jupiter and Saturn in the solar system. As such, U seemed very intriguing and caught our interest.

Mainly because of detector saturation by the bright α Cen, this anonymous object had not been noticed before at any wavelength and its nature was thus undetermined, i.e. whether it was physically associated with α Cen or an object in the fore- or background. Consequently, the object was termed U, meaning unidentified. To gain insight, data from at least another epoch would be required.

In Table 6, the data for the C 2 and C 4 observations are compiled. As previously mentioned, also during C 4 was α Cen observed in all bands. However, the U source would have been outside the primary beam of Band 9 and, hence, no data are available for this source in that band. The identifications are based on positional coincidences across all the bands. In Figure 5, the observations are shown for Bands 8 and 7 in C 2 (left) and C 4 (right), respectively, demonstrating the reliability of this approach. On the right-hand side, the Band 8 and 7 images of 2017 are particularly compelling, as these data were taken on the same day and within 30 minutes: in both data sets is the U source situated exactly in the same place in the sky (see also Table 6).

5.1.1. The proper motion of U

The apparent sky motions of U with time do not allow any meaningful determination of its parallax. Its distance remains therefore unknown, but of course, it is much larger than that of α Cen. The C 2 data for Bands 7, 9 and 8, and the C 4 data for Bands 6, 8 and 7 are collected around essentially the same Right Ascension and displaced by $+0''.2$ in Declination. Therefore, over the course of 1.9 years, any proper motion of U is limited to $\mu_{\alpha} < -15 \text{ mas yr}^{-1}$ and $\mu_{\delta} < 100 \text{ mas yr}^{-1}$. These numbers essentially reflect the astrometric accuracy of the ALMA data. Anyway, these limits are very much different from the proper motion of α Cen, i.e. $\mu_{\alpha} = -3620 \text{ mas yr}^{-1}$ and $\mu_{\delta} = 694 \text{ mas yr}^{-1}$ (Kervella et al. 2016), and we conclude that U is (quasi-)stationary, implying that U is not part of the nearby high-proper-motion α Cen system.

5.2. The SED of U

As shown in Table 6, flux data could be extracted for all bands during C 2, whereas in C 4, the source was not detected in Bands 3 and 4 and, in Band 9, it was outside the field of view. The resulting SED is shown in Fig. 6, together with a regression fit to the logarithmic data. The slope of that line is 2.55 ± 0.14 . If due to thermal emission by dust, an opacity exponent β of about 0.5 would be implied, where $\kappa_{\nu} \propto \nu^{\beta}$. This is similar to the dust

Table 6. ALMA observations of the U source during 2014 - 2017

Date	Bd	ν	R.A. (2000)	Dec. (J2000)	S_ν	δS_ν
yyyy mm dd		GHz	hh mm ss.sss	° ' "	mJy	mJy
2014 07 03	3	97.5	14 39 28.458	-60 49 52.83	0.0554	0.0011
2015 01 18	4	145	14 39 28.539	-60 49 52.79	0.1565	0.0015
2014 12 16	6	233	14 39 28.444	-60 49 53.01	0.592	0.07
2014 07 07	7	343.5	14 39 28.507	-60 49 52.66	1.34	0.4
2015 05 02	8	405	14 39 28.507	-60 49 52.74	3.2	0.5
2014 07 18	9	679	14 39 28.504	-60 49 52.70	6.7	1.3
2016 12 30	6	233	14 39 28.510	-60 49 52.42	0.559	0.09
2017 03 26	8	405	14 39 28.505	-60 49 52.50	1.47	0.6
2017 03 26	7	343.5	14 39 28.505	-60 49 52.50	1.86	0.4
2016 12 19	4	145	< 0.08	1 σ
2017 05 08	3	97.5	< 0.017	1 σ

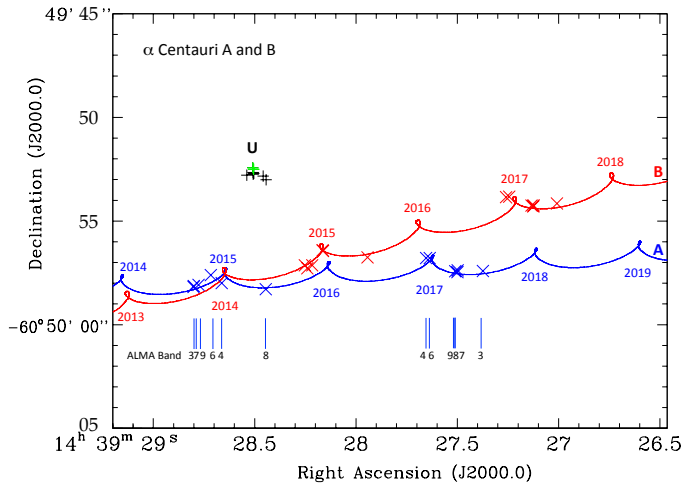


Fig. 4. The displayed $20'' \times 20''$ region shows the ephemerides of the α Cen binary during the two ALMA-observing epochs. α Cen A is shown in blue and B in red. For clarity, the symbols for the observed positions in 2014 to 2017 are much larger than the statistical errors, which are on the milli-arcsecond scale. The ALMA bands for the positions of A are identified below the blue curve. Above both curves, the measured sky positions of the U source are shown as crosses: in black for C2 (2014/15) and in green for C4 (2016/2017).

found in, e.g., the debris disc around β Pic (Liseau et al. 2003), where the dust particles are significantly larger than those found in the diffuse interstellar medium, for which $\beta \sim 2$.

6. Conclusions

We have obtained 2nd epoch data for α Centauri in ALMA-Bands 3, 4, 6, 7, 8 and 9 (92 to 675 GHz). The Band 3 data of ALMA Cycle 4 had to be re-taken due to problems with the phase calibration, and that delayed the analysis. But the main reason for the delay was our discovery that the already published data (Cycle 2) for bands 3 and 4 were faulty: these were based on a flux calibration using Ceres that was eventually abandoned. Unfortunately, we were not made aware of that by the ALMA project, but found out in the course of the analysis of the Cycle 4 data.

Here, we provide a complete re-reduction and analysis. With the aim of assessing the level of chromospheric time variability, the comparison of the results from the earlier C2 campaign with

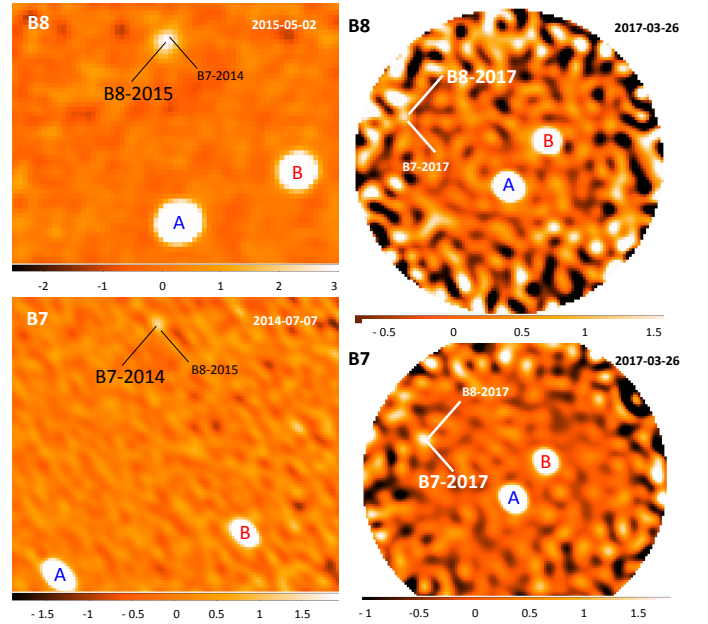


Fig. 5. Left: The relative positions of unidentified sources in the Bands 8 and 7 in the observed C2 images. B8-2015 is the discovery image of the U source, and the position of a corresponding object in the Band 7 observation is indicated (B7-2014). The spatial scale of B 8 is given by the angular distance of α CenA and B, i.e. $\overline{AB} = 4''0$. Below, part of the Band 7 image, where the object B7-2014 is identified, together with the one of the upper frame (B8-2015). In that image, $\overline{AB} = 4''2$ and the units of the intensity, shown along the color scale bar, are mJy/beam. North is up and East is to the left. **Right:** Similar to above, but for the C4 observations. The Band 8 and 7 data have been obtained on the same date (2017-03-26) within half an hour. Consequently, the images of the U source coincide in both frames, as expected. The angular scale is given by $\overline{AB} = 4''2$. The units of the intensity, shown along the color scale bar, are mJy/beam. North is up and East is to the left.

those from C4 casts doubt on the quality of the ALMA data even for the nearest stars to the Sun.

The mysterious object U that was discovered in May 2015, then about $5''$ north of α Cen A, has been re-observed during Cycle 4 in all bands, except in Band 9, where it fell outside the primary beam. These second epoch data were examined in order to establish whether U shared the proper motion of α Cen. It does not. Hence, U is not related to the α Cen system. Nevertheless, U appears to be an interesting object in its own right.

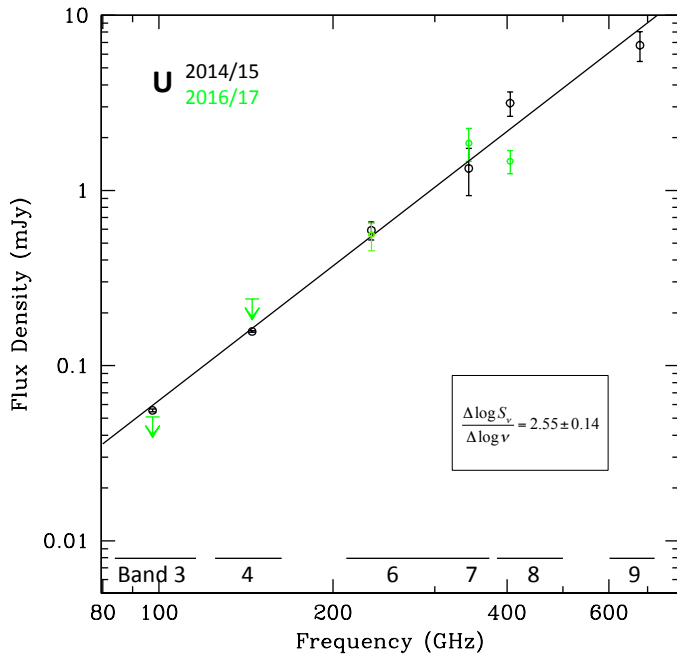


Fig. 6. The observed SED with ALMA of the U source. The C 2 data are shown in black, whereas the C 4 (2016 – 2017) data are in green. The upper limits are 3σ . The inset shows the results of a linear regression fit in log-log space.

Acknowledgements. We are grateful to Drs. Paresh Prema and Steve Bell at the HM Nautical Almanac Office, UK, for their kind help with essential data. We also wish to thank Dr. Sebastien Muller at the Nordic ALMA Regional Centre (ARC node) for his great help with the ALMA data. The Nordic ARC node is funded through Swedish Research Council grant No 2017-00648. Dr. Dirk Petry at the ALMA User Support at ESO assisted with the Ceres calibration issues. This paper makes use of the following ALMA data: ADS/JAO.ALMA#2013.1.00170.S and #2016.1.00441.S. ALMA is a partnership of ESO (representing its member states), NSF (USA), and NINS (Japan), together with NRC (Canada) and NSC and ASIAA (Taiwan), in cooperation with the Republic of Chile. The Joint ALMA Observatory is operated by ESO, AUI/NRAO, and NAOJ.

References

- Butler, B. 2012, ALMA Memo 594
 Kervella, P., Mignard, F., Mérand, A., & Thévenin, F. 2016, A&A, 594, A107
 Liseau, R., Brandeker, A., Fridlund, M., et al. 2003, A&A, 402, 183
 Liseau, R., De la Luz, V., O’Gorman, E., et al. 2016, A&A, 594, A109
 Liseau, R., Vlemmings, W., Bayo, A., et al. 2015, A&A, 573, L4
 Press, W. H., Flannery, B. P., & Teukolsky, S. A. 1986, Numerical recipes. The art of scientific computing